Coğrafi Bilimler Dergisi / Turkish Journal of Geographical Sciences
2026; 24(2): 565-586 DOI: 10.33688/aucbd.1866825
Research Article

HEC-RAS and GIS based flood hazard analysis: A case study of Muş Basin

HEC-RAS ve GIS tabanlı taşkın tehlikesi analizi: Muş Havzası örneği

Ömer Kalın[a], Mehmet Furkan Şener [*a]

[a]İzmir Bakircay University, Faculty of Humanities and Social Sciences, Department of Geography, İzmir/Türkiye

Abstract

Urbanisation, uncontrolled land use, infrastructure and engineering practices that are inconsistent with basin characteristics, and settlement planning that does not consider flood risk alter natural drainage systems, thereby obstructing surface runoff and increasing flood hazards. Due to topography and climatic conditions that intensify flow processes, Eastern Anatolia is, after the Aegean and Eastern Black Sea regions, one of the regions where flood events are frequently observed. The Muş Basin, located in the Eastern Anatolia Region and covering an area of 3.482 km², is one of Turkey's plains most frequently affected by floods. In this study, the flood threat in the Muş Basin was simulated under various discharge scenarios using measured flow data from previous years, a 5-m-resolution Digital Terrain Model (DTM), and the HEC-RAS 1B modelling system. The results indicate that flood depth and flow velocity exhibit significant spatial variability across the basin. In particular, high flood risk has been identified in the vicinity of the settlements of Sungu, Yeroluk, Mercimekkale, and Muratgören, and these findings are spatially consistent with flood events recorded in previous years

Keywords: *HEC-RAS, GIS, Flood, Muş, Türkiye*

Öz

Kentleşme, kontrolsüz arazi kullanımı, havza özellikleriyle uyumsuz şekilde tasarlanan altyapı ve mühendislik uygulamaları ile taşkın riskini dikkate almadan tasarlanan yerleşim planlaması, doğal drenaj sistemlerini değiştirerek yüzeysel akışı engellemekte bu da taşkın tehlikesini artırmaktadır. Topografya ve iklim koşullarının akış süreçlerini yoğunlaştırması nedeniyle, taşkın olaylarının Ege ve Doğu Karadeniz'den sonra sık görüldüğü bölgelerden biri Doğu Anadolu'dur. Doğu Anadolu Bölgesi'nde yer alan 3.482 km² büyüklüğündeki Muş Havzası, Türkiye'de en çok taşkın gözlemlenen ovalardan biridir. Bu çalışmada, Muş Havzası'ndaki taşkın tehdidi; geçmiş yıllara ait ölçülmüş akım verileri, 5 m çözünürlüklü Dijital Arazi Modeli (DTM) ve HEC-RAS 1B modelleme sistemi kullanılarak çeşitli deşarj senaryoları kapsamında simüle edilmiştir. Sonuçlar, taşkın derinliği ve hızının havza genelinde önemli mekânsal farklılıklar gösterdiğini ortaya koymaktadır. Özellikle Sungu, Yeroluk, Mercimekkale ve Muratgören yerleşimleri çevresinde kritik taşkın riskinin yüksek olduğu belirlenmiş olup, bu bulgular geçmiş yıllarda meydana gelen taşkın olaylarıyla uyum göstermektedir.

Anahtar Kelimeler: *HEC-RAS, GIS, Taşkın, Muş, Türkiye*

***Corresponding Author:** mehmetfurkansener@mail.com; furkan.sener@bakircay.edu.tr

Received: 19.01.2026 **Accepted:** 04.06.2026 **Online Published**: 20.09.2026

To Cite: Kalın, Ö., Y., Şener, M.F. (2026). HEC-RAS and GIS based flood hazard analysis: A case study of Muş Basin, *Coğrafi Bilimler Dergisi/ Turkish Journal of Geographical Sciences,* 24(2), 565-586, https://doi.org/10.33688/aucbd.1866825

1. Introduction

Floods are one of the most severe and devastating events globally (De Moel et al., 2009; Kundzewicz et al., 2014; Paprotny et al., 2019), resulting in substantial economic losses and significantly impacting almost 200 million individuals annually (Chaulagain et al., 2023; Costache et al., 2019; Dottori et al., 2016). The Emergency Incidents Database (EM-DAT) reports an average of 170 flood incidents per year from 2003 to 2022, resulting in 5,518 fatalities and affecting 74.6 million individuals annually, both directly and indirectly. The economic loss throughout this 19-year period amounts to 41.1 billion USD (Tin et al., 2024).

Global climate change results in increased frequency and intensity of hydrometeorological events and disasters, leading to irreversible impacts. Human, geomorphological, and atmospheric variables are directly responsible for this situation (Andreadis et al., 2022; Hallegatte et al., 2013; Hirabayashi et al., 2013; Jongman et al., 2012; Özdemir & Akbas, 2025; Rentschler et al., 2023). The ability of a warmer environment to retain more moisture, resulting in sudden, heavy precipitation, is atmospheric in origin; by contrast, elements such as the basins' topographical relief, water retention capacity, and drainage characteristics are geomorphological in origin. Anthropogenic origin is also linked to changes in land use within the riverbed and its environs, channel concretization, poor design, and engineering errors (Lavell et al., 2012; Winsemius et al., 2016). However, over the past 50 years, flooding in Northwestern Europe has intensified and become more severe due to increased fall and winter precipitation driven by growing development demands and ongoing ecological deterioration. In contrast, there have been fewer floods in Southern Europe's medium and large river basins, which have raised concerns about dryness. With inadequate runoff and flood peak curves, flooding in Eastern Europe has become less likely due to increasing evaporation brought on by warmer temperatures and decreased snow cover and snowmelt (Blöschl et al., 2017; Hall et al., 2014).

Türkiye is among the countries most susceptible to floods due to changes in precipitation patterns, frequency, and intensity brought about by global climate change (Kömüşcü & Çelik, 2013; Kümüşçü et al., 1998; Önol & Unal, 2014). Floods happen almost everywhere in Türkiye (Haltas et al., 2021). Furthermore, 12.2% of all catastrophe occurrences in Türkiye are caused by the flood hazard, which is the most devastating event after earthquakes (Koç & Thieken, 2018; Yüksek et al., 2013). 507 buildings were demolished and 62400 structures were seriously damaged as a result of 6069 occurrences that took place between 1900 and 2018 (Ghasemlounia & Utlu, 2021; Öcal, 2019; Wood et al., 2011). Around 7000 flood episodes occurred in Türkiye between 1908 and 2023, according to a study by Akbaş et al. (2025). The Eastern and Western Black Sea Regions, Büyük and Küçük Menderes, Susurluk, and Meriç River Basins are among the most significant areas affected by flooding. According to regional flood occurrences, the Eastern Anatolia Region had the greatest values (average = 1.72, total = 1706) while the Marmara Region had the lowest values (average = 0.40, total = 315) (AFAD, 2020; Karakuş, 2024; TÜİK, 2021). The province with the highest number of flood episodes was Erzurum (mean = 5.23, total = 371). The province's average value was roughly five times higher than Türkiye's average, and it was responsible for 5.87% of all flood hazards in Türkiye (Demir & Kaya, 2020; Özdemir, 2024; Yılmaz & Akbulut, 2019). Similarly, in the province of Muş, a total of 32 flood events(mean ≈ 0.62)were recorded between 1963 and 2015, and widespread inundations occur across the basin floor due to the simultaneous overflow of the Murat and Karasu Rivers and their contributing drainage networks. Despite experiencing hot and dry summers, the region remains highly vulnerable to flooding today because heavy winter snowfall and intense spring rainfall frequently trigger basin-wide flood events (Dölek, 2013; Dölek & Avcı, 2017).

Numerous studies have been conducted on the general geology, tectonics, petroleum geology, volcanology, geochemistry and hydrogeological characteristics of the study area (Baştuğ, 1976; Göncüoğlu & Turhan, 1985; Kurtman & Akkuş, 1971; Özkan, 1981; Robertson, 2002; Soytürk &Baştuğ, 1973; Tarhan, 1991; Uzelli et al., 2021; Ünal, 1970; Wallace, 1968; Yakupoğlu & Erdoğanlı, 2023). Despite this, few studies have examined the hydrographic characteristics of the Muş basin and the resulting floods and inundations. Based on the flood inventory gathered from local media and Provincial Disaster Risk Reduction Plan (AFAD, 2021) report, 48 flood occurrences were identified as having taken place inside the boundaries of the Muş Basin between 1963 and 2025. Between 1963 and 2025, the majority of flood episodes occurred in April. Floods typically occur at these times because April experiences the highest levels of precipitation and snowmelt.

Flood occurrences can be understood in a variety of ways. One of the most important of these techniques is hydraulic modeling, and the depth-velocity and spread parameters that depend on the flood characteristics are play a key role in assessing flood hazards (Al-Hussein et al., 2022; Basnet & Acharya, 2019; Guven et al., 2025; İcaga et al., 2016; Namara et al., 2022; Ogras & Onen, 2020; Peker et al., 2024; Quirogaa et al., 2016). Consequently, based on the current flow scenarios, the depth and, in particular, the inundation situation that arose in the context of previous flood episodes are crucial for identifying and preventing potential future flood-related issues through hydraulic modeling with a more realistic and accurate scenario (Utlu, 2019).

In addition, flood studies worldwide and in Türkiye frequently employ various hydraulic modelling approaches, notably 1D, 2D, and more recently 3D simulations, which differ in spatial resolution, computational complexity, and ability to represent flow dynamics. While 2D models capture lateral flooding patterns throughout floodplains, 1D models effectively simulate longitudinal flow in river channels, and 3D models offer comprehensive insights into vertical velocity and turbulence structures. In this context, flood hazard analysis refers to the methodical assessment of vulnerable locations by measuring variables, including water depth, flow velocity, and inundation extent. The efficacy of these modeling techniques in evaluating spatial variations in flood hazard has been shown by both international studies (Jibhakate et al., 2023; Mani et al., 2014; Patel et al., 2017) and Turkish case studies (Ceribasi & Ceyhunlu, 2021; Durak & Cürebal, 2025; Spor et al., 2025; Taylan & Damçayırı, 2024; Utlu, 2019; Yalcin, 2019; Yalcin, 2020).

In this context, one-dimensional (1D) hydraulic models continue to be commonly used because of their computational efficiency, lower data requirements, and applicability to long river sections. For basin-scale flood hazard assessments, 1D models are regarded as dependable and efficient when accompanied by high-resolution topographic data and suitable roughness parameterization, even though two-dimensional (2D) and three-dimensional (3D) models may depict flow dynamics in more detail. Consequently, integrating a 1D HEC-RAS model with a 5-m-resolution digital terrain model (DTM) and GIS-based spatial analyses provides a strong framework for evaluating flood hazard in the Muş Basin and significantly advances regional flood risk management and spatial planning.

The main objectives of this study are to carry out Hec-RAS 1D (One Dimensional) modelling of flood episodes on the Karasu and Murat Rivers in the Muş Basin using different flow data, to determine the current distribution areas in the basin, and to establish the flood hazard of the Muş Basin based on depth and velocity. Another aim of the study is to reveal the hazard status of the existing land use within the scope of the modelling to be developed.

2. Study Area

The Muş Basin, one of Türkiye's biggest plains, is situated in the country's Eastern Anatolia Region and has long been vulnerable to flooding because of its geographic location (Dölek, 2013). Study area, which covers 3482 km^2, has an extremely hilly and steep terrain. Mount Nemrut, the region's highest peak at 2950 meters, divides the provinces of Bitlis and Muş and constitutes the basin's eastern boundary. In addition, the basin floor is bordered to the north by Üçsırt Mountain (2024 m), to the southwest by Tosun Hill (2819 m) and Kanıbirim Mountain (2444 m), and to the west by Şahin Hill (2678 m) (Figure 1). The basin measures 30 km in width and 80 km in length (Figure 1). Settlements on the study area, which is classified as a young tectonic basin by geomorphology (Göncüoğlu & Turhan, 1985; Uzelli et al., 2021), are often found on the plain floor and nearby.

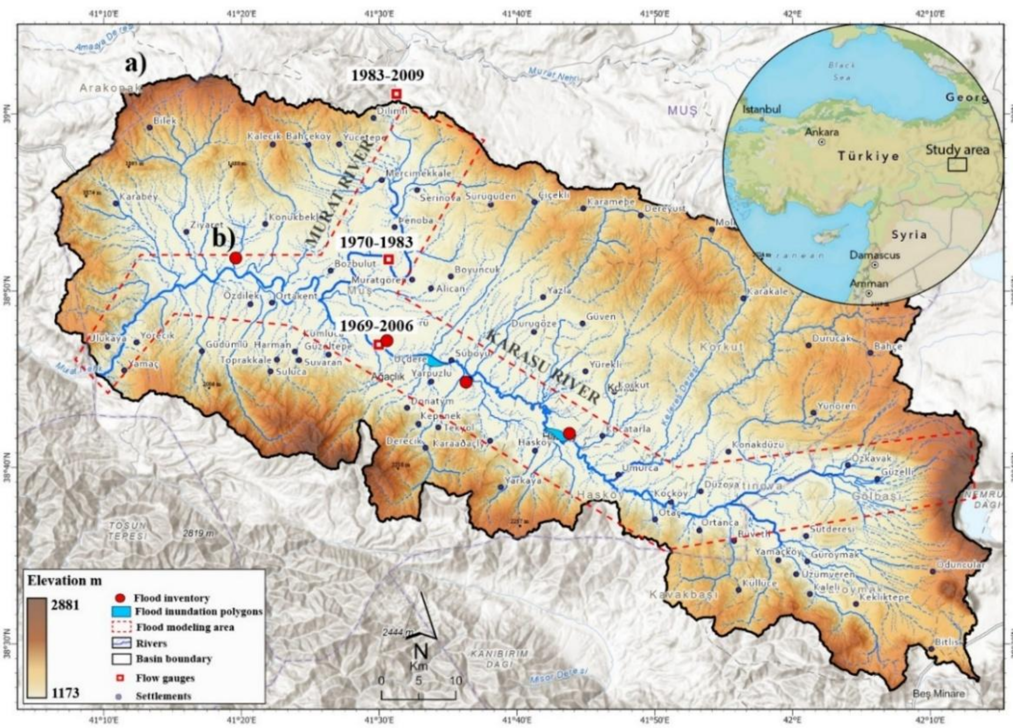

Figure 1. The location map of the study area

Additionally, although many towns, hamlets, and neighborhoods in and around the river corridors are located on high, steep hillslopes rather than on the valley floor, these settlements nevertheless remain exposed to sudden and severe flooding. This risk primarily arises because the steep topography accelerates surface runoff during intense rainfall, causing rapid concentration of flow toward stream channels. As a result, even settlements situated on hillslopes may become exposed to high-velocity flood waves and debris-laden flows under extreme rainfall conditions (Figure 1).

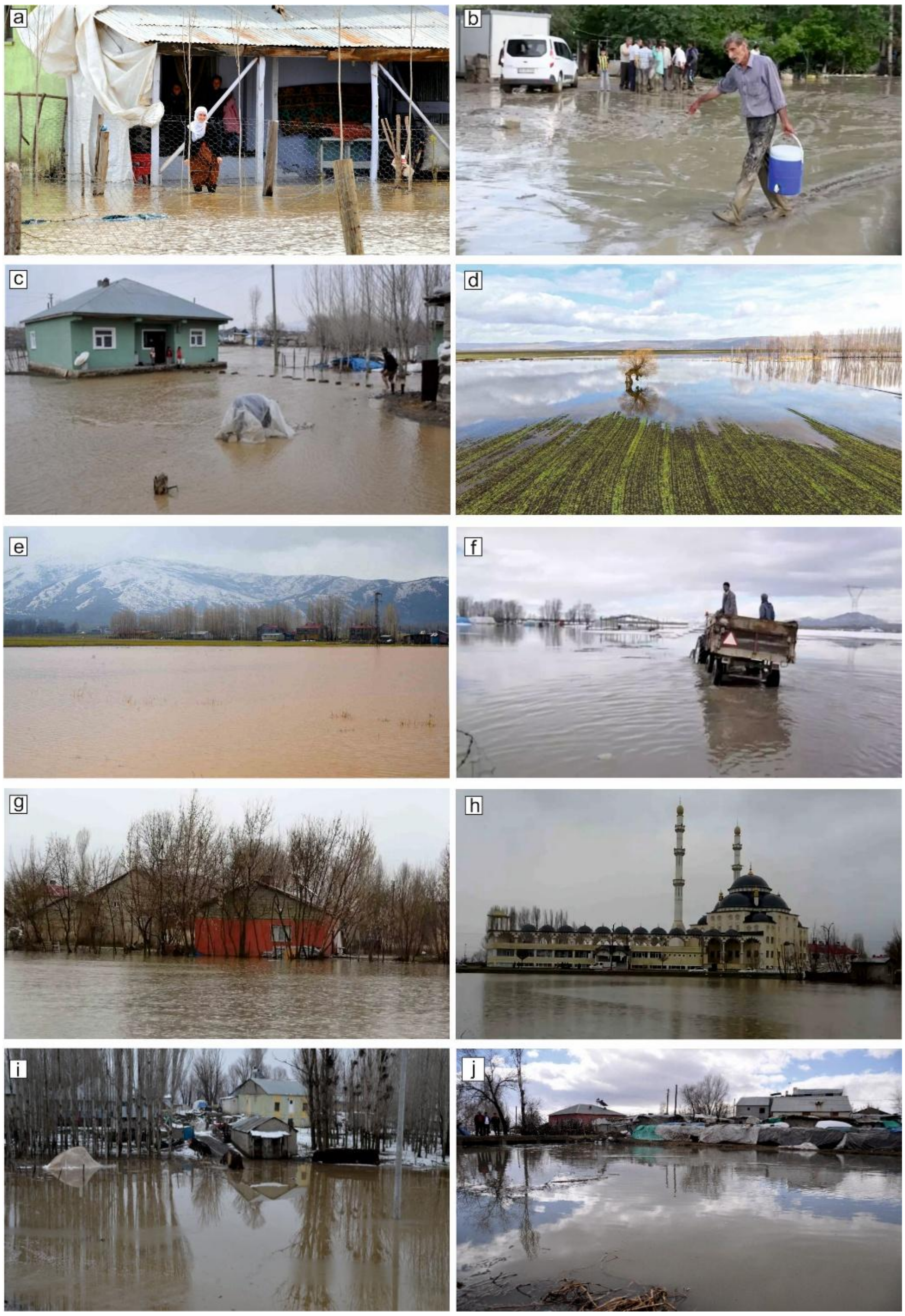

Figure 2. Floods occurring in Muş basin. a. Sungu 2011, b. Korkut 2016, c. Yoncalıöz 2019, d. Düzkışla 2019, e. Çatbaşı 2020, f. Kıyık 2024, g. Center (15 Temmuz Neighbourhood) 2024, h. Hasköy 2024, i. Yeroluk 2024, Koçköy 2024.

The rivers in the east-west extensional geometry of study area have a flow characteristic that corresponds to the slope (MGM, 2021). Throughout the basin, the Murat River runs north-south, whereas the Karasu River flows east-west. In the western part of the basin, these two rivers converge at an elevation of 1245 meters. In this regard, the two major rivers in the basin, the Murat and Karasu, which have numerous tributaries, are the principal rivers responsible for floods observed in the basin. Critical flood episodes have occasionally occurred in various dates and locations within the field (MHRP, 2011) (Figure 2). These floods have caused a great deal of social and economic harm (Dölek 2015, Dölek, 2024).

Historical flood records indicate that the Muş Basin has experienced recurrent floods affecting multiple settlements along the Murat and Karasu river corridors over the past decades (Table 1). Documented flood occurrences between 1963 and 2015 demonstrate that both central districts and surrounding rural settlements have repeatedly been exposed to inundation hazards, resulting in damage to residential areas and infrastructure, livestock losses, and occasional fatalities. Particularly notable are the flood events recorded in 2003 and 2010, which caused loss of life and affected many households, highlighting the socio-economic vulnerability of settlements within the floodplain.

The spatial distribution of historically affected settlements corresponds closely with the flood-prone areas identified by the HEC-RAS hydraulic modelling results presented in this study. This consistency between historical flood inventory data and model-derived inundation extents provides additional qualitative support for the reliability of the flood hazard assessment. Therefore, the historical flood inventory not only demonstrates the long-term recurrence of flooding in the basin but also reinforces the necessity of basin-scale hydraulic modelling for flood risk mitigation and land-use planning.

Table 1. Historical flood events recorded in the Muş Basin and surrounding settlements.

No	District	Settlement	Year	Affected Households	Loss of Life	Other
1	Merkez	Sungu	1963	11		
2	Merkez	Kıyık	1966	15		
3	Merkez	Karaağaç	1969	11		
4	Merkez	Üçdere	1968	5		
5	Hasköy	Yarkaya	1968	15		
6	Korkut	Calaplı	1974	7		
7	Merkez	Şenova	1987			
8	Merkez/Korkut	Karşıyaka	2003	20		
9	Merkez	Derecik, Ilıca	2003		6	
10	Merkez	Kıyıbaşı,	2009			70 livestock losses
11	Merkez	Tüten, Akpınar, Susurağı, Kutlugün	2009			
12	Hasköy	Sungu, Erentepe Beldeleri	2010		1	300 houses affected
13	Sungu	Düzkışla	2011			
14	Merkez,Sungu	Karakuyu	2012			
15	Sungu/Hasköy/ Korkut	Düzkışla,Kocatarla,Gölyazı,Karakale	2013	50		Bridge damage
16	Merkez	Sudurağı	2014			40 livestock losses
17	Merkez	Yoncaöz	2015			Multiple livestock losses

***Source:** From Dölek (2016).

3. Data and Method

The primary climatic type in the Muş basin is "D," which is described as the "Dsa and Dsb" classes of subclimate types, in accordance with the Koppen climate classification (Öztürk et al., 2017; Peel et al., 2007). Furthermore, these values are within the range of the continental Central Anatolian precipitation belt, which is found in high mountainous regions, and the mid-latitude continental climatic type, which has chilly, humid winters (Türkeş & Tatlı, 2011). The raster-based grid climate data type indicates that the total precipitation ranges from 666 to 961 mm and the average annual temperature fluctuates between 3.9 and 10.4 °C (Fick & Hijmans, 2017) (Figure 3 and Figure 4).

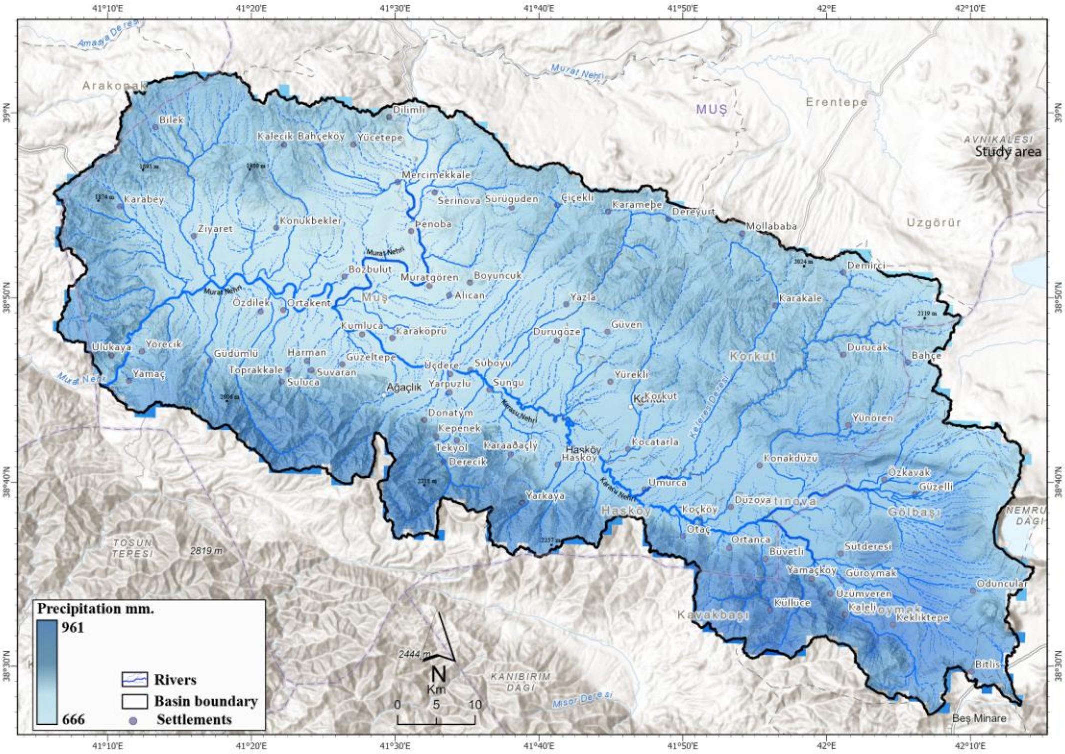

Figure 3: Precipitation distribution map of the study area

***Source:** Modified from Fick & Hijmans (2017).

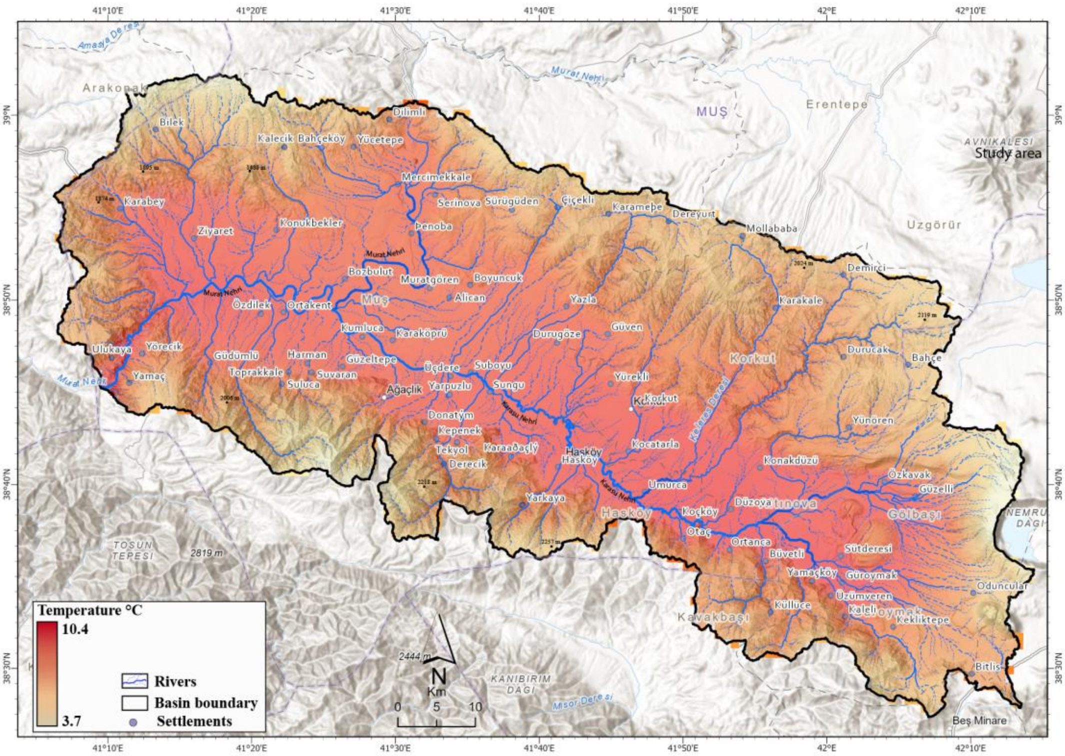

Figure 4: Temperature distribution map of the study area
***Source:** *M*odified from Fick & Hijmans (2017).

3.1. Landcover Data

Manning's N value and land cover types are two of the most crucial pieces of information in flood modeling. Land cover data derived from Sentinel 1 and Sentinel 2 satellite images at 10 m resolution, with a worldwide accuracy of 76.7% (Url-1) (Table 2), provide an essential foundation for calculating Manning's N roughness coefficient and serve as the foundational data set for the hydraulic model. Using Chow (1959), Jain (2000), Sturm (2001), and Akan & Iyer (2021), Manning's N roughness coefficient was determined.

Table 2. Data used in the study

Datasets	Resolution	Source
DTM	5 m	Directorate General for Mapping
Flow Measurements	1969-2006 (year)	Electricity Survey Administration
Land cover	10 m	Worldcover, 2021
Climate data	1 km	WorldClim, 2020

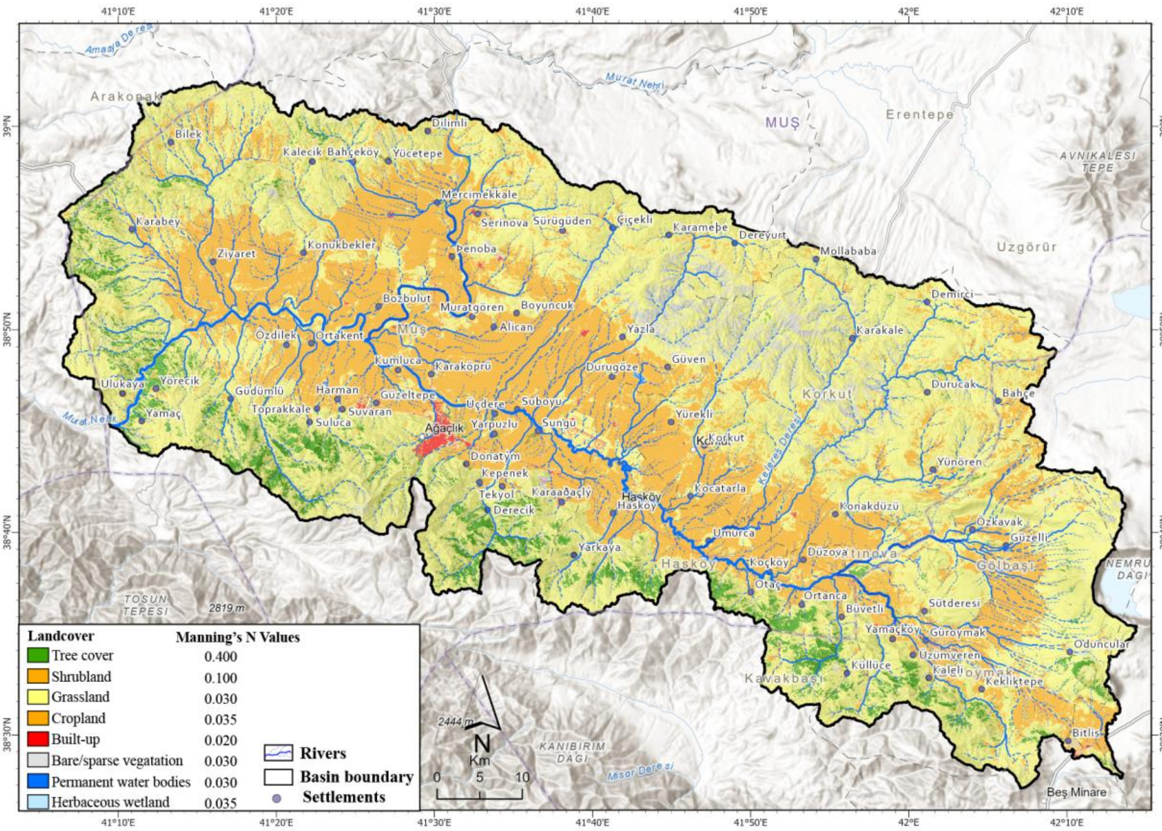

Figure 5. The landcover map and Manning's N values of the study area

As a result, eight distinct land-type classes were found in the region where land-cover data were generated. Wetlands, water bodies, and built-up areas occupy the least area among land classes, whereas grassland and farmland cover the largest area (Figures 5 and 6). All of the research datasets were created using WGS84 UTM-Zone 37 N, the base maps needed to finish the study in the reference system were made using licensed ArcGIS Pro 3.3.0, and hydraulic modeling was done using the open-source Hec-RAS 6.6 application (USACE, 2025).

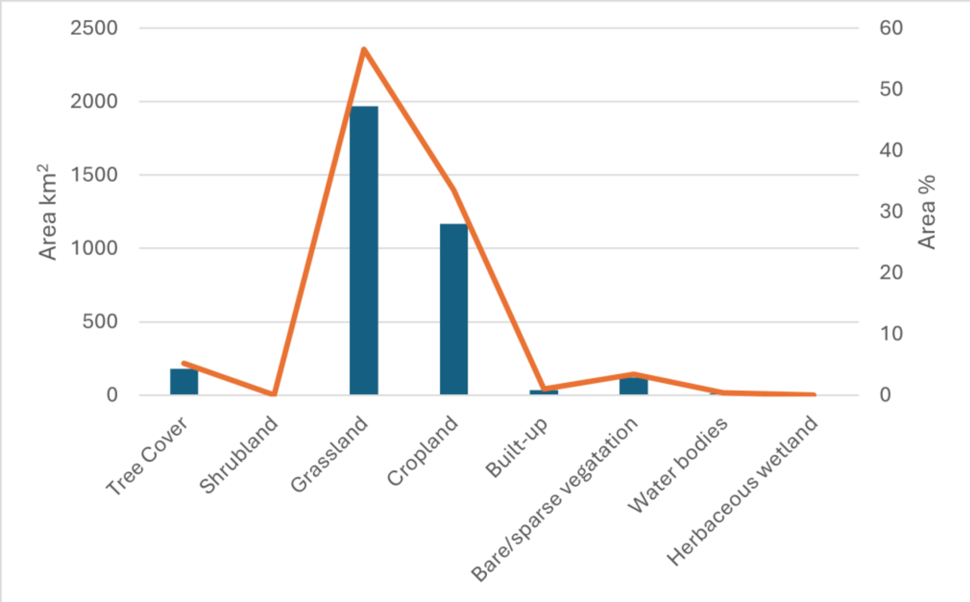

Figure 6. Areal and proportional distribution graph of land cover in the study area

3.2. Methodology

Flood episodes in the Muş basin are influenced by two significant rivers: the Karasu and the Murat. Understanding the flood potential of these two significant rivers and characterizing the hydraulic aspects of flood inundation — depth and velocity — under various scenarios are crucial. In this case, the analysis was based on DTM data at 5 m resolution and land cover data at 10 m resolution. The flowchart shows the steps used to complete the study (Figure 6).

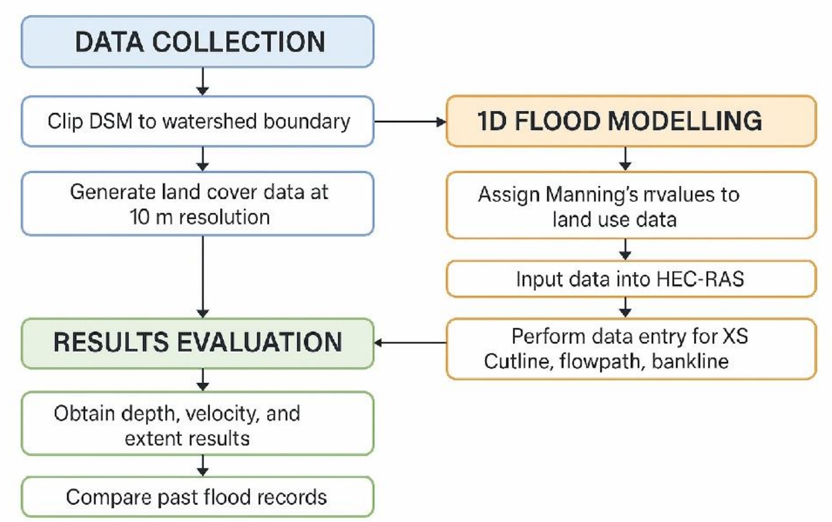

Figure 7. General flowchart of the flood modelling

To produce the datasets, the DTM and land cover data were clipped to the basin boundary. Data entries for the riverbeds to be modeled were generated in the HEC-RAS software environment using XS-Cutline, bankline, and flowpath. Lastly, 1D modeling was performed using the basin's steady flow data under various flow-rate scenarios, based on Electricity Survey Administration data. Current data have been obtained from long-term records of the Electricity Authority Research Institute. However, because data continuity was interrupted at some stations (due to failure to maintain up-to-date records and intermittent outages), reliable frequency analyses could not be produced for each station. Therefore, the minimum, average, and maximum observed flow rates during the measurement period were selected as model inputs.

Flood modeling, which is essential for comprehending the hydrodynamic properties of floods, is mostly done in 1D and 2D (Fijko & Zeleňáková, 2016; Utlu & Özdemir, 2020). Consequently, regions with extremely wide and complex topography are increasingly favoring 1D modeling these days (Alaghmand et al., 2010, Paiva et al., 2011; Schuman et al., 2007). In light of this, modeling was conducted for the 41-kilometer Karasu River and the 55-kilometer Murat River. In the simulated region, there are 60 cross sections in the Murat River and 52 in the Karasu River. Cross-line lengths on the Karasu and Murat rivers range from 6697 to 9885 meters and 5400 to 9004 meters, respectively. Based on the kinetic motion of water across the cross sections produced during 1D hydraulic modeling, the energy equation (1) is essential (USACE, 2016).

$$Z_2 + Y_2 + a_2 \frac{v_2^2}{2_g} = Z_1 + Y \frac{v_1^1}{2_g} + h_e \quad (1)$$

where, Z_1 and Z_2 are topographic surface features (m) located in and around the river, Y_1 and Y_2 are the depths (m) obtained from the hydraulically modelled cross sections, v_1 and v_2 are the average water velocity of the cross sections (m s^{-1}total flow), a_1 and a_2 are coefficients dependent on water velocity, g is gravity (m s^{-2}), h_e is energy loss on the cross sections (Utlu & Özdemir, 2020; Utlu & Ghasemlounia, 2021).

In addition, the energy loss (h_e) of the dynamic model on each cross section is calculated by formula (2).

$$h_e = L\bar{S}f + C \left| a_2 \frac{v_2^2}{2_g} - a_1 \frac{v_1^2}{2_g} \right| \quad (2)$$

where, L is total current value used in the modelling, $\bar{S}f$ is the friction between the cross sections due to the bed inclination, C is the coefficient of contraction and expansion loss (Utlu et al., 2020; Utlu and Özdemir 2020).

Besides, in this study, flood hazard mapping was generated by integrating the depth and velocity outputs obtained from the 1D hydraulic simulations, and the hazard levels were classified according to the criteria proposed by De Moel et al. (2009), which define inundation danger based on combined flow depth–velocity thresholds. Following this approach, four hazard categories were defined according to water depth: Low hazard – dangerous for individuals (<1.25 m); Moderate hazard – dangerous for groups (1.25–2.5 m); High hazard – dangerous for most people (2.5–5 m); and Extreme hazard – dangerous for everyone (>5–20 m). This classification enabled a systematic assessment of spatial flood hazard variations across the basin and provided a consistent framework for interpreting the hydraulic model outputs.

This research deliberately used observed minimum, average, and maximum discharge values rather than statistically calculated recurrence-period flows. Traditional frequency analysis can lead to considerable uncertainty in assessing flood hazard in areas where gaps, inconsistencies, or discontinuities in measurement stations restrict the trustworthiness of long-term hydrological data. In these circumstances, flood behavior is carefully yet realistically represented using a scenario-based modeling technique informed by reported extreme values.

This method enables direct comparison of model outputs with observed flood occurrences and evaluation of the river system's hydraulic response under stress levels reported previously. The use of observed discharge scenarios guarantees that modeling findings for the Muş Basin are grounded in practical evidence rather than theoretical assumptions, since several flood occurrences have been documented there despite scant data from measurement stations.

Furthermore, uncertainties regarding roughness coefficients, cross-sectional spacing, and land surface representation are inherent in all hydraulic models. In this study, these uncertainties were minimized by using high-resolution Digital Terrain Model (DTM) data and assigning Manning roughness coefficients based on land cover. However, the results mainly reflect hydraulic conditions defined under the steady-flow assumption. Time-dependent (unsteady) flow simulations and flood scenarios based on recurrence intervals will help further improve flood hazard assessments and will be addressed in future studies.

4. Results and Discussions

4.1. River Flow Simulation Using HEC-RAS

The hydraulic characteristics of the flood episodes on the Karasu and Murat rivers were analyzed using 1D Hec-Ras modeling. The volume of water discharged into the environment reaches hazardous levels as these rivers increase their capacity to carry water. Flow measurements for these two rivers from 1970 to the present were used to estimate likely flood zones and to compare these estimates with those from previous floods (Figure 8). The lowest, average and highest flow values for Murat River in Muş Basin are 17 m^3/s, 127 m^3/s and 1764 m^3/s, respectively. For the Karasu River, they are likewise 0.2 m^3/s, 24.74 m^3/s, and 410 m^3/s, respectively. These flow values were used to generate a 1D hydraulic model for the Murat River's flow data of 127 and 1764 m^3/s and the Karasu River's flow data of 24.74 m^3/s and 410 m^3/s (Figure 8).

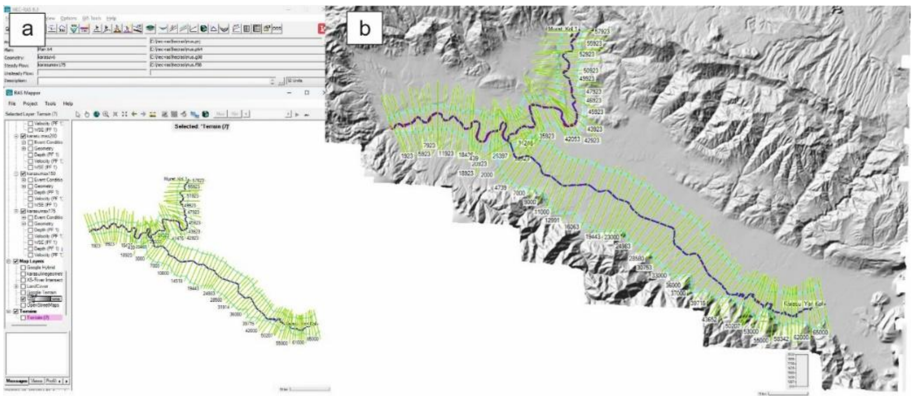

Figure 8. Importing and editing geometric data into Hec Ras software

This modeling was developed for the Muş Basin for the first time, and the flood propagation, based on observed flow data, had varying impacts on the riverbed and adjacent environments. The depth distribution map (Figure 9a) and the flood hazard map (Figure 9b) were built using the daily maximum values because no notable floods were observed in the Murat and Karasu rivers at the daily minimum and average values (Figure 9a and 9b).

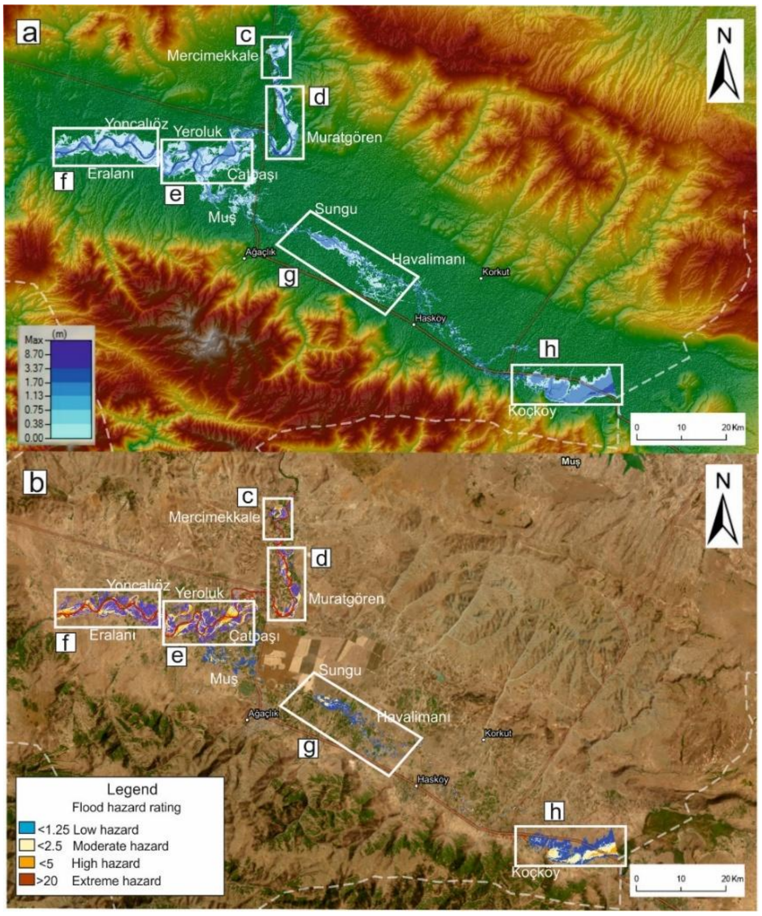

Figure 9. 1764 m³/sec Murat River and 410 m³/sec Karasu River, a. depth distribution map, b. flood hazard map, c. Mercimekkale site, d. Muratgören site, e. Yeroluk and Çatbaşı sites, f. Yoncalıöz and Eralanı sites, g. Sungu site, h. Koçköy site

At the Mercimekkale site, the northern portions are inundated at a flow rate of 1764 m³/sec, as shown by the depth *distribution* map. To better illustrate flood depths and the corresponding elevation differences along the Murat and Karasu rivers, an equal-interval classification method was employed to produce a layered color scale with uniform elevation intervals. Under these conditions, nearby settlements and approximately 650 m² of agricultural land, particularly within meandering sections, are at high risk of flooding. These results indicate a direct threat to both settlements and agricultural productivity in the area (Figures 10a and 10b).

Muratgören site: The flood causes the river level at the Muratgören site to rise to 9 meters, extending 600 meters inland from the beach, with a flow rate of 1764 m³/sec. Floodwaters from the rapidly changing course of the Murat River in the northwestern part of the Muratgören area inundated agricultural lands extending up to the boundaries of Muratgören village, and some makeshift structures were also submerged. Flood control measures need to be examined immediately, as the current drainage systems in this region are insufficient (Figure 10c and 10d).

Kıyık, Bozbulut, Çatbaşı ve Yeroluk site: Kıyık, Bozbulut, Çatbaşı, and Yeroluk are the areas at greatest risk of flooding. In these areas, floodwaters have been observed reaching the boundaries of village houses. Agricultural lands in Bozbulut, Çatbaşı, and Yeroluk were submerged, though the houses remained unharmed. In contrast, approximately 10 houses in Kıyık village were directly affected by the floodwaters. With a flow of 1764 m³/sec, the flood has submerged 65% of Kıyık village and a sizable portion of the villages of Bozbulut and Yeroluk. The water level reaches approximately 8.5 meters and extends approximately 550 meters inland. One of the most notable aspects of the Yeroluk region is the significant impact of flooding on agricultural lands and the ensuing ponding in low-lying regions. These circumstances influence agricultural production and long-term problems. If flood control measures are not put in place at once, there will likely be fatalities and property damage in these areas (Figure 10e and 10f).

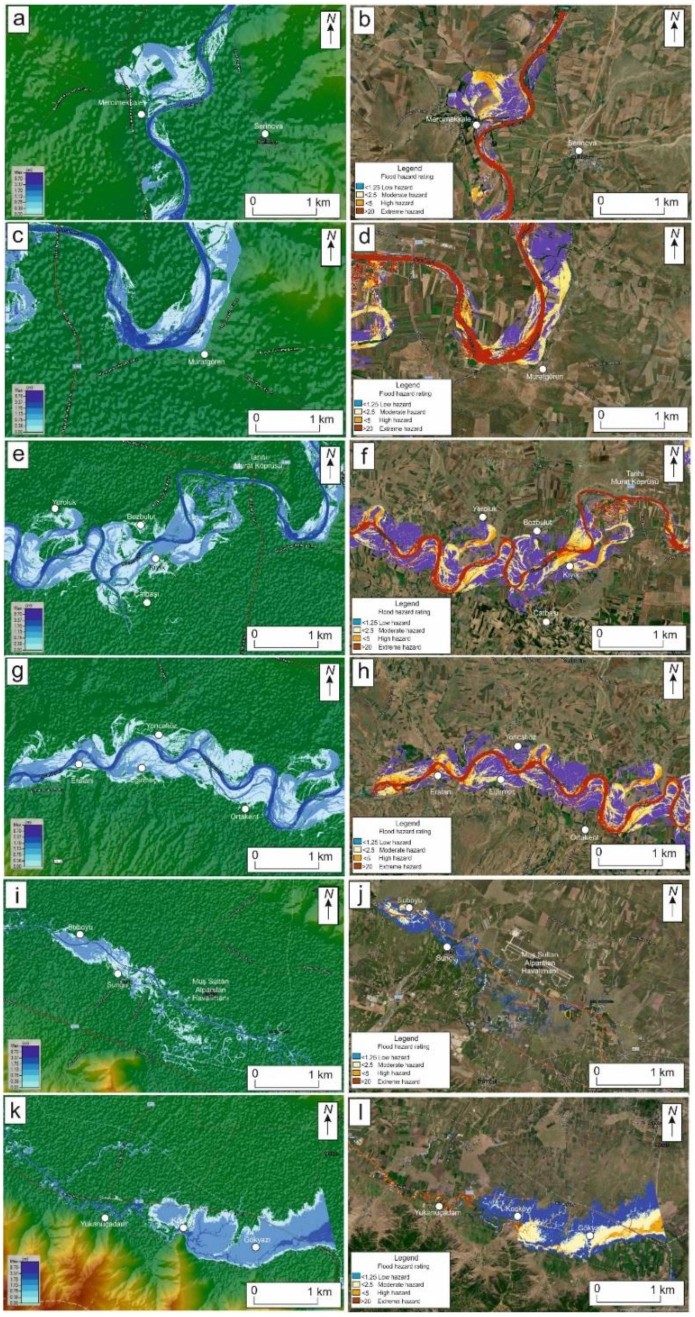

Figure 10. 1D Hec Ras model created with 1764m^3/sec flow rate a. depth distribution , b. flood hazard map of Mercimekkale site; c. depth distribution , d. flood hazard map of Muratgören site; e. depth distribution , f. flood hazard map of Yeroluk and Çatbaşı sites; g. depth distribution , h. flood hazard map of Yoncalıöz and Eralanı sites; i. depth distribution , j. flood hazard map of Sungu site, k. depth distribution , l. flood hazard map of Koçköy site.

Yoncalıöz ve Eralanı site: The Yoncalıöz and Eralanı sites are among the areas most affected by the Murat River. In these locations, agricultural lands were inundated, with the impact more severe than in other areas. In Yoncalıöz, floodwaters primarily submerged farmland, whereas in the Eralanı region, makeshift structures and railway-related buildings located within agricultural fields came into contact with the floodwaters. According to modeling studies of a flood scenario with a flow rate of 1764 m^3/sec, water would rush approximately 600 meters inland from the beach, and water levels would rise up to 7 meters in certain locations. The greatest threats to the region include long-term effects of flooding and ponding in agricultural fields along the direction of flow. Compared to other areas, Yoncalıöz will require more time to drain, which will adversely affect agriculture and infrastructure (Figure 10g and 10h).

The Sungu site is a location on the Karasu River. As a result of flooding from the Karasu River, which flows northwest of Sungu, the village's agricultural lands and structures near the riverbed were inundated. During a flood with a flow rate of 410 m^3/sec, water advanced approximately 200 meters inland from the beach, and water levels rose by 6–7 meters in some locations, despite reclamation work undertaken in the region in 2001. The river's slope allows floodwaters to spread over a wide area and remain for extended periods, potentially causing significant infrastructure damage and major losses to agricultural production (Figure 10i and 10j).

Koçköy site: This area is among the most susceptible to flood damage from the Karasu River, which can inundate a large area. Koçköy, with buildings situated about three meters from the riverbed, is the village adjacent to the Karasu River. Agricultural fields and buildings near the river were identified as at risk from river flooding. Modeling studies based on a flood scenario with a flow rate of 410 m^3/sec indicate that a large percentage of the region is inundated. The river's relatively gentle slope allows floodwaters to move slowly and remain for long periods, creating marshy regions and causing significant losses to agricultural production even where there are no densely populated areas nearby (Figure 10k and 10l).

The modeling findings demonstrate a high degree of agreement between settlements with previously documented flood damage and simulated flood-sensitive locations. Over the past several decades, communities such as Mercimekkale, Muratgören, Yeroluk, and Sungu have experienced frequent flooding, and HEC-RAS models effectively depict these flood-susceptible regions. This consistency validates the applicability of the technique used for flood hazard assessments at the watershed scale and improves the reliability of the model outputs.

Compared with previous GIS-based HEC-RAS studies conducted in other parts of Türkiye, the Muş Basin exhibits flood characteristics typical of broad alluvial plains, primarily fed by snowmelt-driven stream systems. Long-term flooding, significant agricultural damage, and delayed drainage are often key elements of such ecosystems. These findings imply that flood risk reduction methods adopted in the Muş Basin should emphasize not only structural solutions but also land-use planning, early warning systems, and sustainable floodplain management techniques.

4.2. Model Validation Using Sentinel-1 SAR Data

Because continuous streamflow measurements at gauging stations in the Muş Basin were discontinued after 2006, event-specific discharge hydrographs, which are required for conventional hydraulic model validation, could not be obtained for recent flood events. Therefore, an independent spatial validation approach based on Sentinel-1 Synthetic Aperture Radar (SAR) imagery was adopted to evaluate the spatial consistency between the HEC-RAS model outputs and observed flood extents. Sentinel-1 SAR data provide reliable flood extent mapping capability under cloud-independent day-and-night acquisition conditions and are widely used in hydraulic model evaluation studies (Cao et al., 2019; Islam & Meng, 2022; Twele et al., 2016; Uddin et al., 2019).

Sentinel-1 SAR-derived flood extent maps were generated for two major flood events affecting the basin on 5 May 2019 and 19 March 2024, and were compared with the HEC-RAS 1D model outputs representing the maximum discharge scenario (Murat River: 1764 m³/s; Karasu River: 410 m³/s). These two dates were chosen as they align with documented flood events in regional disaster records and correspond to major flooding episodes along the Murat and Karasu river corridors. The comparison was performed at both the basin scale and the pixel level using confusion-matrix-based performance indicators, including the Critical Success Index (CSI), Hit Rate (HR), and False Alarm Rate (FAR).

Under the maximum discharge scenario, the HEC-RAS model estimated a total inundation area of 8,503 ha, including 5,159 ha along the Murat River corridor and 3,387 ha along the Karasu River corridor. Sentinel-1 SAR observations detected 1,041 ha of high-confidence inundation area for the 2019 event and 9,841 ha for the 2024 event. A detailed comparison between model outputs and SAR-derived inundation extents is presented in Table 3.

Table 3. Comparison of HEC-RAS 1D Model Outputs and Sentinel-1 SAR-Derived Flood Extent for the 19 March 2024 and 5 May 2019 Events

Parameter	2024	2019
HEC-RAS Total Inundation Area	8,503 ha	8.503 ha
SAR High-Confidence Inundation Area	9,841 ha	9.841 ha
TP – Agreement Area (Both methods)	8,470 ha	8.470 ha
FP – HEC-RAS Only (Model overprediction)	32 ha	32 ha
FN – SAR Only (Model underprediction)	9,808 ha	9.808 ha
Hit Rate	99.60%	%99,6
False Alarm Rate	0.40%	%0,4
CSI (Critical Success Index)	0.463	0,463

Pixel-level comparison of the 5 May 2019 flood event revealed a strong spatial correspondence between the modelled inundation extent and SAR observations (CSI = 0.889, HR = 90.4%). Of the total 8,503 ha of flood extent predicted by the HEC-RAS model, 8,344 ha (98.1%) overlapped with SAR-detected flooded areas, indicating a high level of agreement between simulated and observed flood patterns.

For the 19 March 2024 flood event, moderate spatial correspondence was obtained (CSI = 0.463; HR = 46.3%). However, an 8,470 ha (99.6%) of the modelled inundation extent was independently confirmed by Sentinel-1 SAR observations, demonstrating that the HEC-RAS model accurately represents flood-prone areas along the main river corridors.

The very low False Alarm Rates obtained for both flood events (0.4–1.9%) indicate that the HEC-RAS model rarely overestimates inundation areas, and therefore provides a reliable representation of flood-susceptible regions within the basin.

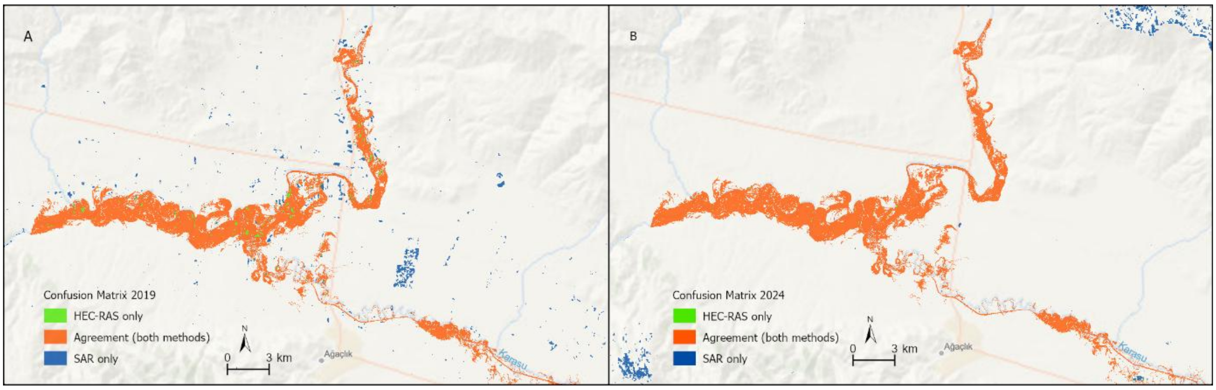

Figure 11. Validation map of HEC-RAS 1D model outputs (orange) in the Muş Basin against Sentinel-1 SAR-derived flood inundation extents (blue) for (a) 5 May 2019 and (b) 19 March 2024.

As shown in Figure X, the HEC-RAS 1D model outputs exhibit strong spatial agreement with Sentinel-1 SAR-derived flood extents for both the 2019 and 2024 events, particularly along the Murat and Karasu river corridors. However, the SAR imagery captures extensive lateral flood propagation across the alluvial plain that the 1D model does not represent.

5. Conclusions

This study focuses on the Muş Basin in Eastern Anatolia, which, at 3,482 km², is one of the largest basins in the region. The principal tributaries of the Euphrates River, the Murat and Karasu rivers, flow through the Muş Basin. The people and agricultural regions on the basin floor have always been at serious risk from floods that occur in the Muş Basin during wet seasons. Although floods have decreased as a result of the Karasu River's restoration efforts over the past ten years, they still occur because the drainage networks supplying the major tributary have not been restored. In this context, Hec-Ras analysis and existing DTM data at 5 m resolution were used to calculate potential flood-prone areas and associated hazards at the foot of the Muş basin. Based on the minimum, average, and maximum flow values, three distinct models were created for the basin bottom. The Murat River has an intraday flow value of 17 m^3/sec at its lowest, 127 m^3/sec at its average, and 1764 m^3/sec at its greatest. The Karasu River has an intraday flow value of 0.2 m^3/sec at its lowest, 24.74 m^3/sec at its average, and 410 m^3/sec at its peak.

The HEC-RAS 1D flood modeling indicates that, while the Murat and Karasu rivers do not pose a significant flood hazard under minimum and average flow conditions, both residential and agricultural areas are at serious risk under maximum flow conditions. The HEC-RAS 1D flood modeling indicated that the volume of floodwater discharging from the riverbed was deemed hazardous in the flood scenario characterized by a flow rate of 1764 m^3/sec in the Murat River. The floodwaters range from 16 cm to 2.11 m. This flood level raises the possibility of both property damage and fatalities. The areas most at risk from flooding include Mercimekkale, Şenoba, Bozbulut, Çatbaşı, Kıyık, Muratgören, Yeroluk, Taşoluk, Eğirmeç, Yoncalıöz, and Eralanı. HEC-RAS 1D flood research indicates that the Karasu River and its tributaries experience floods when the flow rate reaches 410 m3/sec. According to the model, the floodwaters in the riverbed of the Karasu River range from 19 cm to 2.75 m. In addition, the communities of Sungu, Suboyu, Kumluca, Çatbaşı, and Koçköy are among the most severely affected.

The steps needed to lower the risks, which are based on scenarios built using the collected data and the conceptual models developed, are outlined below. Based on this,

1. The reclamation project for the Karasu River began at Çatbaşı and proceeded to Yukarıüçadam village; however, no reclamation work was carried out beyond that point. Improvements are needed in this area. The communities along the Karasu River are at risk of flooding when its flow increases noticeably.

2. The drainage networks that feed the Karasu River and pass through the Hasköy region have not undergone sufficient renovation. For instance, the Çayhendeği Stream in the drainage network flooded in 2024. Consequently, the bearing walls of the Çayhendeği Stream need to be raised and widened.

3. In the reclamation works carried out on the Murat River between Mercimekkale and Murat Goren, and between the villages of Kıyık and Eralanı, embankments were constructed by piling soil. In the case of a river with a high potential flow rate, these precautions are inadequate. Although settlements are not located close to the bed, floods still cause damage to the barns and agricultural regions. Rehabilitation works between Mercimekkale and Murat Goren, as well as between the villages of Kıyık and Eralanı, are therefore crucial.

4. In addition, safety measures should be taken as the houses on the banks of Çatbaşı Village, in the northern part of Eralanı Village, in the eastern part of Örenoba Village, and in the northern part of Muratgören Village, all of which are located at the confluence of Karasu and Murat Rivers, are at risk of flooding.

5. In the Muş Basin, the flows of the Murat and Karasu rivers and of the main drainage systems that feed them should be measured regularly. Unmanned aerial vehicles should be used for modelling studies and for monitoring riverbeds and drainage beds in flood-risk areas.

Overall, the Sentinel-1 SAR–based validation demonstrates that the HEC-RAS 1D hydraulic model reproduces the main spatial patterns and longitudinal extent of flood inundation in the Muş Basin with high reliability, particularly along the Murat and Karasu river corridors, as evidenced by strong overlap and low false alarm rates.

Despite the robust results obtained from 1D hydraulic modeling, this study has some limitations. The analyses are based on steady-state flow conditions and observed discharge scenarios, and may not fully reflect the temporal variability of flood hydrographs during extreme events. Moreover, the modeling methodology does not specifically account for future changes in stream shape, land use, or climate.

Nonetheless, the results provide a solid basis for understanding the current flood risk in the Muş Basin. Future research will enhance flood risk assessments and aid in the creation of comprehensive flood management plans by incorporating time-dependent (unsteady) flow simulations, climate change estimates, and higher-resolution topographic data into the model. Consequently, the 1D flood models created with the HEC-RAS software show overlap between the likely flood zones and historical flood areas. The current methodology uses the recorded minimum, average, and maximum flow values to produce a cautious evaluation of flood-prone locations.

However, the use of statistical flow values derived from different return periods in future studies will complement the current findings and increase the reliability of the estimates. Therefore, this study will serve as a model for other regions investigating flood risk and as a reference for future research.

Ethical and Author Declarations / *Etik ve Yazar Beyanları*

Graduate Thesis Information

This study is based on the Master's thesis by Ömer Kalın, the first author, which was completed at the Department of Geography, İzmir Bakırçay University.

Lisansüstü Tez Bilgileri

Bu çalışma, İzmir Bakırçay Üniversitesi Coğrafya Bölümü'nde tamamlanan ve 1 nolu yazar olan Ömer Kalın'ın Yüksek Lisans tezinden üretilmiştir.

Authors' Contributions

In this study, Ö.K. was responsible for the research design, data collection, and analysis, while M.F.Ş. handled the research design, methodology, writing, and editing phases.

Yazarların Katkı Oranları

Ö.K. araştırma tasarımı, veri toplama ve analiz aşamalarını, M.F.Ş. araştırma tasarımı, metodoloji, yazım ve düzeltme aşamalarını gerçekleştirmiştir.

Ethical Statement

The authors confirm that this study was conducted in accordance with the principles of academic research and publication ethics, and that all sources used are appropriately cited.

Araştırma Etiği Beyanı

Bu çalışmanın hazırlanma sürecinde bilimsel araştırma ve yayın etiği ilkelerine riayet edilmiş; yararlanılan tüm kaynaklar eksiksiz biçimde kaynakçada belirtilmiştir..

Conflict of Interest

The author declare that they have no commercial or financial relationships that could give rise to a conflict of interest during the preparation and publication of this study.

Çıkar Çatışması

Yazarlar, bu çalışmanın hazırlanması ve yayımlanması sürecinde çıkar çatışması oluşturabilecek herhangi bir ticari veya finansal ilişki içinde olmadığını beyan eder.

Ethical Approve

This study does not require ethical committee approval, and the data used were obtained through a literature review/published sources.

Etik Onay

Bu çalışma, etik kurul izni gerektirmeyen nitelikte olup kullanılan veriler literatür taraması/yayınlanmış kaynaklar üzerinden elde edilmiştir.

Yapay Zekâ Kullanımı

Çalışma kapsamında yapay zeka uygulamalarından yararlanılmamıştır.

Use of Artificial Intelligence

No artificial intelligence applications were used in the course of this study.

Acknowledgment

We would like to express our sincere gratitude to Mustafa Utlu and Şevki Danacıoğlu for their valuable contributions and assistance in preparing this article and creating the maps.

Bilgilendirme

Bu makalenin hazırlanmasında ve haritaların oluşturulmasındaki değerli katkıları ve yardımları için Mustafa Utlu ve Şevki Danacıoğlu'na içten teşekkürlerimizi sunarız.

References

AFAD (2020). Türkiye Afet Müdahale Planı. Afet ve Acil Durum Yönetimi Başkanlığı Yayını. Ankara.

AFAD (2021). İl Afet Risk Azaltma Planı (IRAP). Muş Valiliği, İl Afet ve Acil Durum Müdürlüğü, Muş, Türkiye.

Akan, A. O., & Iyer, S. S. (2021). *Open channel hydraulics*. Butterworth-Heinemann, CRC Press.

Alaghmand, S., bin Abdullah, R., Abustan, I., & Vosoogh, B. (2010). GIS-based river flood hazard mapping in urban area (a case study in Kayu Ara River Basin, Malaysia). *International Journal of Engineering and Technology, 2*(6), 488-500. https://doi.org/10.7763/IJET.2010.V2.172

Al-Hussein, A. A., Khan, S., Ncibi, K., Hamdi, N., & Hamed, Y. (2022). Flood analysis using HEC-RAS and HEC-HMS: a case study of Khazir River (Middle East—Northern Iraq). *Water, 14*(22), 3779. https://doi.org/10.3390/w14223779

Akbaş, A., Görüm, T., & Özdemir, H. (2025). Türkiye'de taşkınların FlooDOT tabanlı incelenmesi ve farklı veri kaynaklarının mekânsal karşılaştırılması. *Turkish Journal of Civil Engineering, 36*(6).

Andreadis, K. M., Wing, O. E. J., Colven, E., Gleason, C. J., Bates, P. D., & Brown, C. M. (2022). Urbanizing the floodplain: global changes of imperviousness in flood-prone areas. *Environmental Research Letters, 17*(10), 104024. https://doi.org/10.1088/1748-9326/ac9288

Basnet, K., & Acharya, D. (2019). Flood Analysis at Ramghat, Pokhara, Nepal Using HEC-RAS. Technical Journal, 1(1), 41-53.

Baştuğ, C. (1976). Bitlis napının stratigrafisi ve Güneydoğu Anadolu sütur zonunun evrimi. *Yeryuvarı ve İnsan, 1*(3), 55-61.

Blöschl, G., Hall, J., Parajka, J., Perdigão, R.A., Merz, B., Arheimer, B., Aronica, G.T., Bilibashi, A., Bonacci, O., Borga, M., & Čanjevac, I. (2017). Changing climate shifts timing of European floods. *Science, 357*(6351), pp.588-590. https://doi.org/10.1126/science.aan2506

Cao, H., Zhang, H., Wang, C., & Zhang, B. (2019). Operational flood detection using Sentinel-1 SAR data over large areas. *Water, 11*(4), 786. https://doi.org/10.3390/w11040786

Ceribasi, G., & Ceyhunlu, A. I. (2021). Generation of 1D and 2D flood maps of Sakarya river passing through Geyve district of Sakarya city in Turkey. *Natural Hazards, 105*(1), 631-642. https://doi.org/10.1007/s11069-020-04327-8

Chaulagain, D., Ram Rimal, P., Ngando, S. N., Nsafon, B. E. K., Suh, D., & Huh, J.-S. (2023). Flood susceptibility mapping of Kathmandu metropolitan city using GIS-based multi-criteria decision analysis. *Ecological Indicators, 154*, 110653. https://doi.org/10.1016/j.ecolind.2023.110653

Chow, V.T. (1959). *Open-channel hydraulics*: New York, McGraw-Hill, 680 p.

Costache, R., Pham, Q.B., Sharifi, E., Linh, N.T.T., Abba, S.I., Vojtek, M., Vojteková, J., Nhi, P.T.T. & Khoi, D.N. (2019). Flash-flood susceptibility assessment using multi-criteria decision making and machine learning supported by remote sensing and GIS techniques. *Remote Sensing, 12*(1), 106. https://doi.org/10.3390/rs12010106

Demir, G., & Kaya, A. (2020). Türkiye'de sel afetlerinin mekânsal dağılımı ve risk analizi. *Türk Coğrafya Dergisi, 75*, 15–30.

De Moel, H. D., van Alphen, E. J., Aerts, J. C. (2009). Depth distribution s in Europe–methods, availability and use. *Natural Hazards and Earth System Sciences, 9*(2), 289-301. https://doi.org/10.5194/nhess-9-289-2009

Dottori, F., Salamon, P., Bianchi, A., Alfieri, L., Hirpa, F. A., & Feyen, L. (2016). Development and evaluation of a framework for global flood hazard mapping. *Advances in Water Resources, 94*, 87-102. https://doi.org/10.1016/j.advwatres.2016.05.002

Dölek, İ. (2013). Muş'ta yaşanan sel ve taşkinlara neden olan doğal faktörlerin analizi. *Marmara Coğrafya Dergisi*, (28), 408-422.

Dölek, İ. (2015). Sungu beldesi ve yakin çevresinde (Muş) sel ve taşkina duyarli alanlarin belirlenmesi. *Marmara Coğrafya Dergisi, (31),* 258-280.

Dölek, İ. (2016). Muş ilinde doğal tehlike kaynağı olarak sel ve taşkınlar, sel ve taşkına duyarlı alanların analizi, Muş ili için doğal tehlike kaynakları, 81-129, https://doi.org/10.13140/RG.2.1.3354.2000

Dölek, İ., & Avci, V. (2024). Muş ilinin sel ve taşkin duyarlilik haritalarinin oluşturulması. *The Journal of Academic Social Science, 44*(44), 190-204.

Durak, M., & Cürebal, İ. (2025). HEC-RAS tabanlı 2 boyutlu taşkın tehlike çalışması: Bahadınlı ve Karadere (Burhaniye – Balıkesir). *Jeomorfolojik Araştırmalar Dergisi*(*15*), 126-149. https://doi.org/10.46453/jader.1777585

Fick, S.E., & Hijmans, R.J. (2017). WorldClim 2: new 1km spatial resolution climate surfaces for global land areas. *International Journal of Climatology, 37* (12): 4302-4315. https://doi.org/10.1002/joc.5086

Fijko, R., & Zeleňáková, M. (2016). The HEC RAS model of regulated stream for purposes of flood risk reduction. Journal of *Civil Engineering, 11*(1), 59-70.

Ghasemlounia, R., & Utlu, M. (2021). Flood prioritization of basins based on geomorphometric properties using principal component analysis, morphometric analysis and Redvan's priority methods: A case study of Harşit River basin. *Journal of Hydrology, 603*, 127061. https://doi.org/10.1016/j.jhydrol.2021.127061

Göncüoğlu, M.C., & Turhan, N. (1985). Bitlis metamorfik kuşağının orta bölümünün temel jeolojisi, MTA Raporu, Rapor No: 7707 (yayımlanmamış), Ankara.

Guven, D. S., Yenigun, K., Isinkaralar, O., & Isinkaralar, K. (2025). Modeling flood hazard impacts using GIS-based HEC-RAS technique towards climate risk in Şanlıurfa, Türkiye. *Natural Hazards, 121*(3), 3657-3675. https://doi.org/10.1007/s11069-024-06977-w

Haltas, I., Yildirim, E., Oztas, F., & Demir, I. (2021). A comprehensive flood event specification and inventory: 1930–2020 Turkey case study. *International Journal of Disaster Risk Reduction, 56*, 102086. https://doi.org/10.1016/j.ijdrr.2021.102086

Hall, J., Arheimer, B., Borga, M., Brázdil, R., Claps, P., Kiss, A., Kjeldsen, T.R., Kriaučiūnienė, J., Kundzewicz, Z.W., Lang, M., & Llasat, M.C. (2014). Understanding flood regime changes in Europe: a state-of-the-art assessment. *Hydrology and Earth System Sciences, 18*(7), 2735-2772. https://doi.org/10.5194/hess-18-2735-2014

Hallegatte, S., Green, C., Nicholls, R. J., & Corfee-Morlot, J. (2013). Future flood losses in major coastal cities. *Nature Climate Change, 3*(9), 802–806. https://doi.org/10.1038/nclimate1979

Hirabayashi, Y., Mahendran, R., Koirala, S., Konoshima, L., Yamazaki, D., Watanabe, S., Kim, H., & Kanae, S., (2013). Global flood risk under climate change. *Nature climate change, 3*(9), pp.816-821. https://doi.org/10.1038/nclimate1911

Islam, M. T., & Meng, Q. (2022). An exploratory study of Sentinel-1 SAR for rapid urban flood mapping on Google Earth Engine. *International Journal of Applied Earth Observation and Geoinformation, 113*, 103002. https://doi.org/10.1016/j.jag.2022.103002

İcaga, Y., Tas, E., & Kilit, M. (2016). Flood inundation mapping by GIS and a hydraulic model (HEC RAS): A case study of Akarcay Bolvadin subbasin, in Turkey. *Acta Geobalcanica, 2*(2), 111-118.

Jain, S.C. (2000). *Open-Channel Flow*, John Wiley & Sons. INC., New York, ISBN: 978-0-471-35641-7

Jibhakate, S. M., Timbadiya, P. V., & Patel, P. L. (2023). Flood hazard assessment for the coastal urban floodplain using 1D/2D coupled hydrodynamic model. *Natural Hazards, 116*(2), 1557-1590. https://doi.org/10.1007/s11069-022-05731-y

Jongman, B., Ward, P. J., & Aerts, J. C. (2012). Global exposure to river and coastal flooding: Long term trends and changes. *Global Environmental Change, 22*(4), 823-835. https://doi.org/10.1016/j.gloenvcha.2012.07.004

Karakuş, E. (2024). Türkiye'de İklim Değişikliği Bağlamında Taşkın Afetlerinin Bölgesel Dağılımı. *İklim ve Afet Araştırmaları Dergisi, 2*(1), 45–62.

Koç, G., & Thieken, A. H. (2018). The relevance of flood hazards and impacts in Turkey: What can be learned from different disaster loss databases? *Natural Hazards, 91*, 375-408. https://doi.org/10.1007/s11069-017-3132-8

Kömüşcü, A. Ü., & Çelik, S. (2013). Analysis of the Marmara flood in Turkey, 7–10 September 2009: an assessment from hydrometeorological perspective. *Natural Hazards, 66*(2), 781-808. https://doi.org/10.1007/s11069-012-0518-2

Kömüşçü, A. Ü., Erkan, A., & Çelik, S. (1998). Analysis of meteorological and terrain features leading to the Izmir flash flood, 3-4 November 1995. *Natural Hazards, 18*(1), 1–25. https://doi.org/10.1023/A:1008061614781

Kurtman, F., & Akkuş, M.F. (1971). Doğu Anadolu'daki ara basenler ve bunların petrol olanakları. *MTA Dergisi, 77,* 1-10.

Kundzewicz, Z.W., Kanae, S., Seneviratne, S.I., Handmer, J., Nicholls, N., Peduzzi, P., Mechler, R., Bouwer, L.M., Arnell, N., Mach, K. & Muir-Wood, R. (2014). Flood risk and climate change: global and regional perspectives. *Hydrological Sciences Journal, 59*(1), 1-28. https://doi.org/10.1080/02626667.2013.857411

Lavell, A., Oppenheimer, M., Diop, C., Hess, J., Lempert, R., Li, J. & Myeong, S. (2012). Managing the risks of extreme events and disasters to advance climate change adaptation. A special report of working groups I and II of the intergovernmental panel on climate change (IPCC), 3,.25-64.

Mani, P., Chatterjee, C., & Kumar, R. (2014). Flood hazard assessment with multiparameter approach derived from coupled 1D and 2D hydrodynamic flow model. *Natural Hazards, 70*(2), 1553-1574. https://doi.org/10.1007/s11069-013-0889-8

MGM (2021). Türkiye'de Gözlenen Aşırı Hava Olayları Raporu 2021. Meteoroloji Genel Müdürlüğü Yayını, Ankara.

MHRP (2011). Murat Havzası Rehabilitasyon Projesi Fizibilite Raporu, Türkiye Cumhuriyeti Orman ve Su İşleri Bakanlığı, Ankara.

Namara, W. G., Damisse, T. A., & Tufa, F. G. (2022). Application of HEC-RAS and HEC-GeoRAS model for flood inundation mapping, the case of Awash bello flood plain, upper Awash River Basin, oromiya regional state, Ethiopia. *Modeling Earth Systems and Environment, 8*(2), 1449-1460. https://doi.org/10.1007/s40808-021-01167-x

Ogras, S., & Onen, F. (2020). Flood Analysis with HEC-RAS: A Case Study of Tigris River. *Advances in Civil Engineering, 2020*(1), 6131982. https://doi.org/10.1155/2020/6131982

Patel, D. P., Ramirez, J. A., Srivastava, P. K., Bray, M., & Han, D. (2017). Assessment of flood inundation mapping of Surat city by coupled 1D/2D hydrodynamic modeling: a case application of the new HEC-RAS 5. *Natural Hazards, 89*(1), 93-130. https://doi.org/10.1007/s11069-017-2956-6

Peel, M. C., Finlayson, B. L., & McMahon, T. A. (2007). Updated World map of the Köppen-Geiger climate classification. *Hydrology and Earth System Sciences Discussions, 4*(2), 439-47. https://doi.org/10.5194/hess-11-1633-2007

Peker, İ. B., Gülbaz, S., Demir, V., Orhan, O., & Beden, N. (2024). Integration of HEC-RAS and HEC-HMS with GIS in flood modeling and flood hazard mapping. *Sustainability, 16*(3), 1226. https://doi.org/10.3390/su16031226

Paprotny, D., Morales-Nápoles, O., Vousdoukas, M. I., Jonkman, S. N., & Nikulin, G. (2019). Accuracy of pan-European coastal depth distribution ping. *Journal of Flood Risk Management, 12*(2), 1–16. https://doi.org/10.1111/jfr3.12484

Quirogaa, V. M., Kurea, S., Udoa, K., & Manoa, A. (2016). Application of 2D numerical simulation for the analysis of the February 2014 Bolivian Amazonia flood: Application of the new HEC-RAS version 5. *Ribagua, 3*(1), 25-33. https://doi.org/10.1016/j.riba.2015.12.001

Rentschler, J., Avner, P., Marconcini, M., Su, R., Strano, E., Vousdoukas, M., & Hallegatte, S. (2023). Global evidence of rapid urban growth in flood zones since 1985. *Nature, 622*(7981), 87-92. https://doi.org/10.1038/s41586-023-06468-9

Robertson, A.H. (2002). Overview of the genesis and emplacement of Mesozoic ophiolites in the Eastern Mediterranean Tethyan region. *Lithos, 65*(1-2), 1-67. https://doi.org/10.1016/S0024-4937(02)00160-0

Schumann, G., Matgen, P., Hoffmann, L., Hostache, R., Pappenberger, F., & Pfister, L. (2007). Deriving distributed roughness values from satellite radar data for flood inundation modelling. Journal of Hydrology, 344(1-2), 96-111. https://doi.org/10.1016/j.jhydrol.2007.06.027

Sturm, T. W. (2001). *Open channel hydraulics* (Vol. 1, p. 1). New York: McGraw-Hill.

Tarhan, N. (1991). Hınıs-Varto-Karlıova (Erzurum-Muş-Bingöl) dolayındaki Neojen volkanitlerinin jeolojisi ve petrolojisi. *Maden Tetkik ve Arama Dergisi, 113*, 45-60.

Taylan, E. D., & Damçayırı, D. (2024). 2D hydrodynamic model for flood analysis in Kinikli Stream Basin (Tekirdağ, Türkiye). *Iranian Journal of Science and Technology, Transactions of Civil Engineering, 48*(4), 2691-2707. https://doi.org/10.1007/s40996-023-01332-9

Tin, D., Cheng, L., Le, D., Hata, R., & Ciottone, G. (2024). Natural disasters: A comprehensive study using EMDAT database 1995–2022. *Public Health, 226*, 255-260. https://doi.org/10.1016/j.puhe.2023.11.026

TÜİK (2021). Çevresel İstatistikler: Meteorolojik Afet Verileri 2021. Türkiye İstatistik Kurumu, Ankara.

Türkeş, M., & Tatlı, H. (2011). Use of the spectral clustering to determine coherent precipitation regions in Turkey for the period 1929–2007. *International Journal of Climatology, 31*(14), 20552067. https://doi.org/10.1002/joc.2212

Twele, A., Cao, W., Plank, S., & Martinis, S. (2016). Sentinel-1-based flood mapping: a fully automated processing chain. *International Journal of Remote Sensing, 37*(13), 2990-3004. https://doi.org/10.1080/01431161.2016.1192701

Uddin, K., Matin, M. A., & Meyer, F. J. (2019). Operational flood mapping using multi-temporal Sentinel-1 SAR images: A case study from Bangladesh. *Remote Sensing, 11*(13), 1581. https://doi.org/10.3390/rs11131581

Utlu, M. (2019). *Farklı çözünürlüklü veri kaynaklarına bağlı taşkın tehlike analizi: Biga Çayı Havzası örneği.* [Doktora tezi, İstanbul Üniversitesi]. (Yayınlanmamış), Ulusal Tez Merkezi.

Utlu, M., & Özdemir, H. (2020). How much spatial resolution do we need to model a local flood event? Benchmark testing based on UAV data from Biga River (Turkey). *Arabian Journal of Geosciences, 13*(24), 1293. https://doi.org/10.1007/s12517-020-06282-3

Utlu, M., Şimşek, M., & Öztürk, M. Z. (2020). 1D taşkın modellemeleri açısından Topo Dem ve Alos Dsm verilerinin karşılaştırılması: Alara Çayı Örneği. *Ege Coğrafya Dergisi, 29*(2), 161-177.

Utlu, M., & Ghasemlounia, R. (2021). Flood prioritization watersheds of the Aras River, based on geomorphometric properties: Case study Iğdır Province. *Jeomorfolojik Araştırmalar Dergisi,* (6), 21-40.

USACE (2016). Hydrologic Engineering Center, HEC-RAS, River Analysis System Hydraulic Reference Manual. US Army Corps of Engineers, Davis, CA.

USACE (2025). PL 84-99 Advaced Measures, Post-Wildfire Hazard Assessment, 2025 Eaton Fire, County of Los Angeles, California, May 2025, US Army Corps of Engineers, Los Angeles District, Draft Report, 435p.

Uzelli, T., Şener, M. F., Dölek, İ., Baba, A., Sözbilir, H., & Dirik, R. K. (2021). Structural controls and hydrogeochemical properties of geothermal fields in the Vartoregion, East Anatolia. *Turkish Journal of Earth Sciences, 30*(9), 1076-1095. https://doi.org/10.3906/yer-2105-18

Ünal, A. (1970). Muş bölgesi 1: 25 000 ölçekli Erzurum J 47 c4, Muş K 47 b4, c1, c2 paftalarının detay petrol etüdü, MTA Raporu, Rapor No: 4754 (yayımlanmamış), Ankara.

Soytürk, N., & Baştuğ, C. (1973). Kozluk-Baykan yöresi jeoloji raporu, TPAO Raporu, Rapor No: 795 (yayınlanmamış), Ankara.

Spor, P., Paşa, Y., & Doğan, E. (2025). Evaluation of simulation results of hec-ras coupled 1d/2d and 2d modeling approaches through scenario-based analysis. *Water, 17*(8), 1163. https://doi.org/10.3390/w17081163

Öcal, A. (2019). Natural Disasters in Turkey: Social and economic perspective. *International Journal of Disaster Risk Management, 1*(1), 51–61.

Önol, B., & Unal, Y. S. (2014). Assessment of climate change simulations over climate zones of Turkey. *Regional Environmental Change, 14*(5), 1921–1935. https://doi.org/10.1007/s10113-014-0598-6

Özdemir, T. (2024). Erzurum ili örneğinde taşkın tehlikesi ve kırılganlık analizi. *Doğu Anadolu Coğrafya Dergisi, 30*(1), 25–40.

Özdemir, H., & Akbas, A. (2025). Evaluating the capability of UAV-Derived DEMs for flood hazard analysis. *Physical Geography, 46*(3), 175-195. https://doi.org/10.1080/02723646.2024.2371988

Öztürk, M.Z., Çetinkaya, G., & Aydın, S. (2017). Köppen-Geiger iklim sınıflandırmasına göre Türkiye'nin iklim tipleri. *Coğrafya Dergisi, 35*, 17-27.

Paiva, R.C., Collischonn, W., & Tucci, C.E. (2011). Large scale hydrologic and hydrodynamic modeling using limited data and a GIS based approach. *Journal of Hydrology, 406*(3-4), 170-181. https://doi.org/10.1016/j.jhydrol.2011.06.019

Wallace, R.E. (1968). Earthquake of August 19, 1966, Varto area, eastern Turkey. *Bulletin of the Seismological Society of America, 58*(1), 11-45. https://doi.org/10.1785/BSSA0580010011

Winsemius, H.C., Aerts, J.C., Van Beek, L.P., Bierkens, M.F., Bouwman, A., Jongman, B., Kwadijk, J.C., Ligtvoet, W., Lucas, P.L., Van Vuuren, D.P. & Ward, P.J. (2016). Global drivers of future river flood risk. *Nature Climate Change, 6*(4), pp.381-385. https://doi.org/10.1038/nclimate2893

Wood, E.F., Roundy, J.K., Troy, T.J., Van Beek, L.P.H., Bierkens, M.F., Blyth, E., de Roo, A., Döll, P., Ek, M., Famiglietti, J. & Gochis, D. (2011). Hyperresolution global land surface modeling: Meeting a grand challenge for monitoring Earth's terrestrial water. *Water Resources Research, 47*(5). https://doi.org/10.1029/2010WR010090

Yakupoğlu, T., & Erdoğanlı, K. (2023). Whole Rock and Clay Mıneralogy of Early Mıocene Sedımentary Rocks Outcroppıng In The Northeast Of Korkut (Muş-Türkiye). Eskişehir Technical University Journal of Science and Technology A-Applied Sciences and Engineering, 24, 17-32.

Yalcin, E. (2019). Two-dimensional hydrodynamic modelling for urban flood risk assessment using unmanned aerial vehicle imagery: A case study of Kirsehir, Turkey. *Journal of flood risk management,* 12, e12499. https://doi.org/10.1111/jfr3.12499

Yalcin, E. (2020). Assessing the impact of topography and land cover data resolutions on two-dimensional HEC-RAS hydrodynamic model simulations for urban flood hazard analysis. *Natural Hazards, 101*(3), 995-1017. https://doi.org/10.1007/s11069-020-03856-6

Yılmaz, M., & Akbulut, M. (2019). Doğu Anadolu Bölgesi'nde sel olaylarinin coğrafi dağilimi üzerine bir inceleme. *Afet ve Risk Dergisi, 5*(2), 120–135.

Yüksek, Ö., Kankal, M., & Üçüncü, O. (2013). Assessment of big floods in the Eastern Black Sea Basin of Turkey. *Environmental Monitoring and Assessment, 185*(1), 797–814. https://doi.org/10.1007/s10661-012-2592-3